Amr Abuzer*, Ady Naber, Simon Hoffmann, Lucy Kessler, Ramin Khoramnia, and Werner Nahm

Investigation on Non-Segmentation Based Algorithms for Microvasculature Quantification in OCTA Images

Abstract: Optical Coherence Tomography Angiography (OCTA) is an imaging modality that provides three-dimensional information of the retinal microvasculature and therefore promises early diagnosis and sufficient monitoring in ophthalmology. However, there is considerable variability between experts analysing this data. Measures for quantitative assessment of the vasculature need to be developed and established, such as fractal dimension. Fractal dimension can be used to assess the complexity of vessels and has been shown to be independently associated with neovascularization, a symptom of diseases such as diabetic retinopathy. This investigation assessed the performance of three fractal dimension algorithms: Box Counting Dimension (*BCD*), Information Dimension (*ID*), and Differential Box Counting (*DBC*). Two of those, *BCD* and *ID*, rely on previous vessel segmentation. Assessment of the added value or disturbance regarding the segmentation step is a second aim of this study. The investigation was performed on a data set composed of 9 in vivo human eyes. Since there is no ground truth available, the performance of the methods in differentiating the Superficial Vascular Complex (SVC) and Deep Vascular Complex (DVC) layers apart and the consistency of measurements of the same layer at different time-points were tested. The performance parameters were the ICC and the Mann-Whitney U tests. The three applied methods were suitable to tell the different layers apart and showed consistent values applied in the same slab. Within the consistency test, the non-segmentation-based method, *DBC*, was found to be less accurate, expressed in a lower ICC value, compared to its segmentation-based counterparts. This result is thought to be due to the *DBC*'s higher sensitivity when compared to the other methods. This higher sensitivity might help detect changes in the microvasculature, like neovascularization, but is also more likely prone to noise and artefacts.

Keywords: Differential Box Counting, OCTA images, Fractal Dimensions.

1 Introduction

Optical Coherence Tomography Angiography (OCTA) is a non-invasive imaging technique used to diagnose and monitor diseases such as diabetic retinopathy and age-related macular degeneration [1]. In contrast to the lower resolution of the gold standard of microvasculature imaging [2], fluorescein angiography, OCTA allows for layer wise assessment of high-resolution three-dimensional data within the retina and choroid.

OCTA itself assesses the variance of consecutive Optical Coherence Tomography (OCT) scans of the eye. The main cause of variation in subsequent OCT scans is assumed to be due to moving particles, such as erythrocytes, within the retina and the choroid. OCTA data is divided into different slabs following the anatomic structure of the blood vessels in the eye. These are named the Superficial Vascular Complex (SVC), the Deep Vascular Complex (DVC), and the choriocapillaris layer. The SVC and DVC layers are found within the retina, and the choriocapillaris layer is found within the choroid [3].

For any objective assessment of OCTA data, a quantification metric is needed. One such metric is fractal dimensions, a concept introduced in 1951 to describe the complexity of geometric shapes and mathematical functions of irregular shape or form [4]. The fractal dimension of microvasculature describes how thoroughly the pattern fills the space it is in. It was shown that the fractal dimension increases as new vessels form in the process of neovascularization [5]. This measure has been

---

*Corresponding author: Amr Abuzer: Institute of Biomedical Engineering, Karlsruhe Institute of Technology, Karlsruhe, Germany, email: publications@ibt.kit.edu

Ady Naber, Simon Hoffmann, Werner Nahm: Institute of Biomedical Engineering, Karlsruhe Institute of Technology, Karlsruhe, Germany.

Lucy Kessler: Eye Clinic, University Hospital Heidelberg, Heidelberg, Germany, email: LucyJoanne.Kessler@med.uni-heidelberg.de

Ramin Khoramnia: Universitätsklinikum, Heidelberg, Germany, email: Ramin.Khoramnia@med.uni-heidelberg.de

used to assess the complexity of microvasculature, including in fluorescein angiography, where it was shown to be independently associated with neovascularization which is then associated with diabetic retinopathy [6].

There are several ways to assess fractal dimensions. Some require a skeletonised OCTA image, which requires segmentation as a precursor. Differential Box Counting, however, is a fractal dimension measurement that does not require a segmentation step.

This investigation aimed to assess fractal dimension values derived from multiple algorithms to investigate their consistency and their robustness.

2 Materials and Methods

Due to the inaccessability of a ground truth, the following criteria were assessed to get an impression of the algorithms' repeatibility and specifitivity:

1. The repeatability of each algorithm given the same slab at a short time difference
2. The separability between different slabs at the same time point

Initially, 232 images of 58 patient eyes were provided, with varying image quality. For each eye, two subsequent OCTA images were taken with less than a five-minute difference between them. Given this short time between the OCTA data acquisitions, no anatomical changes in the patient's retina should take place. Following this, the FD values extracted from this data should be close.

For each OCTA dataset, an SVC and DVC image can be extracted. Non-ideal images were excluded, giving a final image count of 36 images for 9 eyes.

Due to the patient's motion between the two scans, slight misalignments can be seen between the SVC and DVC en face projections from time-point 1 and 2. Thus, a
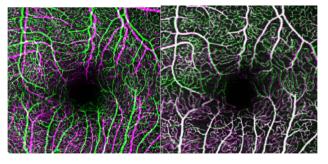

Figure 1: Given is the registration process. Here the purple and green images denote the SVC slabs at the two-time images. The left image is the pair before registration and the right image is the pair after registration.

registration based on Styner et al. [7] which is implemented in commercially available software toolboxes [8] ensured that a vessel comparison was valid between the two subsequent images (see figure 1). The matrix transformations of the images were allowed in rotation, translation, and scaling.

For the segmentation-based methods, a segmentation then a skeletonization of the images was applied. For the non-segmentation-based method, a Sobel filter was applied in the x and y directions to find the magnitude of the gradient for both OCTA images. This was done to normalize the grey values and reduce the grey value variability between the two images.

Quantification Methods

Three fractal dimension methods were used:

1. Box Counting Dimension (BCD)
2. Information Dimension (ID)
3. Differential Box Counting (DBC)

For the implementation of the BCD and the ID methods, take a Boolean square matrix of size $M*M$ that corresponds to the pixel dimensions of the image. The image is then split down into square grids of side lengths $s*s$.

As introduced in *Fractal Dimensions of Networks* [9], BCD is defined by the formula:

$$BCD \equiv \lim_{s \to 0} \frac{\log B(s)}{\log 1/s}$$

BCD, denotes the box-counting dimension; s is the side length of each square grid; $B(s)$ defines the number of images where an intersection between the object, which is given by the value 1, and the grids exist. For quantization accuracy, the side lengths are defined as the factors of M, and a measurement of $B(s)$ is taken for multiple different s trials [9]. Finally, a regression line is drawn between every log $B(s)$ and log $1/s$, with the slope denoting BCD.

As introduced in *Fractal Dimensions of Networks* [9], ID is defined by the formula:

$$ID \equiv -\lim_{s \to 0} \frac{H(s)}{\log s}$$

Similarly, given the same scenario earlier, the information dimension, ID, can also calculate the fractal dimension. Here, s denotes the side length of the square grids, and $H(s)$ denotes the entropy of finding a set number of 1s in a grid. Here the entropy, also called Shannon's entropy, is given by the formula:

$$H(s) = -\sum_s p_s \log p_s$$

An introduction to entropy in information theory as given by Shannon is given in *Fractal Dimensions of Networks* [9].

Again, for quantization accuracy, the side lengths are defined as the factors of *M*, and the *H(s)* of multiple *s* trials is measured [9]. A regression line is drawn between every *H(s)* and *log s,* with the slope of the line denoting *ID*.

DBC, as introduced by Sarkar et. al [10], is defined on the grey value space of the image and thus does not require a prior segmentation. Here, space is defined on *M*M*G* where *M* defines the side lengths of the square image and *G* defines the maximum grey value of the image. A grid is used to measure the fractal dimension of the image; the grid also lies in the third dimension *G*. Therefore, the dimensions of the boxes that define the grid are given by *s*s*s′* where *s′* is a proportionality factor described by:

$$\frac{M}{s} = \frac{G}{s'}$$

s′ describes the height prescribed for every box. The box-counting on each column is then given by the formula:

$$n(i,j) = l - k + 1$$

Here *n(i,j)* is the number of boxes counted in the column *(i,j)*, *l* is the box number given for the maximum grey value within *(i,j)*, and *k* is the box number for the minimum grey value within *(i,j)* [10].

Finally, the total number of boxes counted is given by:

$$N = \sum n(i,j)$$

Here the same procedure done previously with *ID* and *BCD* is done with *DBC*, where *s* is given by the factors of *M*, and the *N* is calculated for multiple *s* trials. Finally, linear regression is done between log *N* and log *1/s*. Due to quantization errors, the method described by Lieu et al. [11] was used to account for known errors in the *DBC*. Errors include undercounting the number of boxes, *n*, due to sharp grey value intensity changes in the images and overcounting due to the definition of *n(i,j)*.

Note the range of each fractal dimension method. Since *DBC* is applied in three-dimensional space, the curve that is being measured should lie between 2.0 and 3.0, where 3.0 denotes a very rough surface [10]. In contrast, after a segmentation process, the curve being measured lies in two-dimensional space thus the expected range of fractal dimensions lies between 1.0 and 2.0.

Statistical Methods

The intraclass correlation coefficient (ICC), two-way mixed effects, and the Mann-Whitney U test were used to assess repeatability of the same slab at two images and the separability of different slabs at the same images, respectively.

The two-way mixed effects ICC is given by the formula [12]:

$$ICC(A,1) = \frac{MS_R - MS_E}{MS_R + (k-1)MS_E + \frac{k}{n}(MS_C - MS_E)}$$

For either SVC or DVC, a matrix is given with rows denoting measurement of all 9 eyes, and columns denoting the different observations of the same eye, at either t_1 or t_2. Here, ICC*(A,1)*, denotes the ICC of two-way mixed effects; MS_R denotes the mean square for the rows; MS_E is the mean square error; MS_C is the mean square for the columns; *k* is the number of observations per eye; *n* is the number of eyes observed [12].

3 Results

The results are visualized in the boxplots in figures 2 and 3. The Mann-Whitney U tests between the SVC slabs at t_1 and t_2 and DVC slabs at t_1 and t_2 of all the methods was found to be ≤ 0.005. The ICC values of all the methods for both layers were > 0.8, however the ICC values of the *BCD* and *ID* were both >0.9, whereas the ICC values of the *DBC* was found to be between 0.82-0.84.
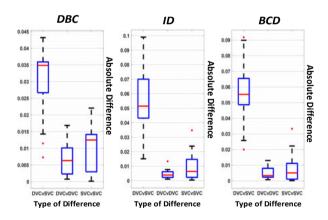

Figure 2: Boxplots visualizing the difference in the fractal dimensions of every method. DVCvDVC denotes the difference in fractal dimension between two DVC images of a given eye. SVCvSVC denotes the difference in fractal dimensions between two SVC images of a given eye. SVCvDVC denotes the difference between the fractal dimensions of SVC and DVC of a given eye. It was used as a reference to compare SVCvSVC and DVCvDVC boxplots. The boxplots show the medians and interquartile of the distributions.
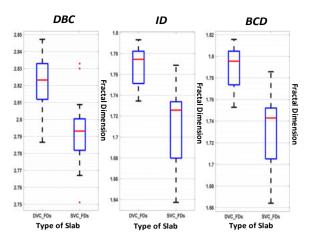
Figure 3: Boxplots visualizing the fractal dimensions of every method. DVC_FDs shows the median and interquartile distribution of the DVC. SVC_FDs shows the median and interquartile distribution of the SVC.

4 Discussion

ICC values > 0.8 and P-values < 0.05 were considered statistically significant.

The results show that the *BCD* and *ID* performed better in comparison to the *DBC*, in separability of measurements of different layers at the same time point and repeatability of measurements of the same layer at different time points.

It is thought that the changes in intensity between the OCTA images could be a possible cause for the higher deviation of error in the *DBC* calculation. Whereas variances in intensity in OCTA have a lower effect, only affecting the calculation for critical pixels just at the threshold, on the segmentation-based methods as they measure the fractal dimension of the two-dimensional geometry in the segmented image.

Artefacts in the OCTA image itself could be another cause for the higher error deviation in the *DBC* as artefacts result in higher intensity values when compared to many neighboring vessels. This leads to a tendency of overcounting artefacts in the *DBC* whereas artefacts and neighboring vessels are counted equally in the segmentation-based methods.

5 Conclusion and Outlook

The *DBC* has been shown to have a lower ICC value within the consistency assessment. This was assumed to be due to sensitivity of *DBC* to artefacts in the image and intensity differences, possibly noise, between the subsequent images.

Therefore, methods such as averaging multiple en-face OCTA images, as outlined by Uji et al. [13], could create

consistent intensity values in subsequent OCTA images and therefore improve the reliability of information for quantification. This method can also attenuate the possible problems caused by motion artefacts.

If variances and artefacts in the OCTA are attenuated, this perceived sensitivity to changes could turn the drawbacks of *DBC* into an advantage since it is more sensitive to changes in the microvasculature, like changes due to neovascularization.

Author Statement

References

[1] J. F. Bille, High resolution imaging in microscopy and ophthalmology : new frontiers in biomedical optics. Springer, 2019.

[2] de Barros Garcia, Jose Mauricio Botto, David Leonardo Cruvinel Isaac, and Marcos Avila. "Diabetic retinopathy and OCT angiography: clinical findings and future perspectives." International journal of retina and vitreous 3.1 (2017): 1-10.

[3] Rocholz, Roland, et al. "SPECTRALIS optical coherence tomography angiography (OCTA): principles and clinical applications." *Heidelb Eng Acad* September (2018): 1-10.

[4] H. Meinhardt, "Models of biological pattern formation," New York, vol. 118, 1982.

[5] Daxer, Albert. "The fractal geometry of proliferative diabetic retinopathy: implications for the diagnosis and the process of retinal vasculogenesis." Current eye research 12.12 (1993): 1103-1109.

[6] Daxer, Albert. "Characterisation of the neovascularisation process in diabetic retinopathy by means of fractal geometry: diagnostic implications." Graefe's archive for clinical and experimental ophthalmology 231.12 (1993): 681-686.

[7] Styner, M., C. Brechbuehler, G. Székely, and G. Gerig. "Parametric estimate of intensity inhomogeneities applied to MRI." *IEEE Transactions on Medical Imaging.* Vol. 19, Number 3, 2000, pp. 153-165

[8] MATLAB registration.optimizer.OnePlusOneEvolutionary Copyright 2011-2015 The MathWorks, Inc. Documentation (accessed on 07.09.2021): https://www.mathworks.com/help/images/ref/registration.optimizer.onepluson eevolutionary.html

[9] E. Rosenberg, Fractal dimensions of networks. Springer, 2020

[10] N. Sarkar and B. B. Chaudhuri, "An efficient approach to estimate fractal dimension of textural images," Pattern recognition, vol. 25, no. 9, pp. 1035–1041, 1992.

[11] Y. Liu, L. Chen, H. Wang, et al., "An improved differential box-counting method to estimate fractal dimensions of gray-level images," Journal of visual communication and Image Representation, vol. 25, no. 5, pp. 1102–1111, 2014

[12] McGraw, Kenneth O., and Seok P. Wong. "Forming inferences about some intraclass correlation coefficients." Psychological methods 1.1 (1996): 30.

[13] Uji, S. Balasubramanian, J. Lei, et al., "Impact of multiple en face image averaging on quantitative assessment from optical coherence tomography angiography images," Ophthalmology, vol. 124, no. 7, pp. 944–952,